J. Water Environ. Nanotechnol., 7(2): 155-169 Spring 2022

ORIGINAL RESEARCH PAPER

Synthesis, Characterization and Photocatalytic Application of $MgZrO_3$@Fe_2O_3@ZnO Core-Shell Oxide for the Degradation Nigrosine Dye

Y. R. Shelke, V. D. Bobade, D. R. Tope, J. A. Agashe and A. V. Borhade*

Department of Chemistry, Research Centre, HPT Arts and RYK Science College, Nasik (MS), INDIA (Affiliated to Savitribai Phule Pune University)

Received:2022-02-20 Accepted: 2022-04-09 Published: 2022-05-01

ABSTRACT

Water pollution is one of the serious main global concerns that affect humans and numerous people die due to various diseases caused by contaminated water because of the toxic and carcinogenic nature of dyes in effluents. It is essential to develop an efficient and effective method for wastewater treatment using a highly active and reusable catalyst. Herein we report heterogeneous catalyst $MgZrO_3$@Fe_2O_3@ZnO nanoparticles by sol-gel approach. They were characterized by UV-visible diffused reflectance spectroscopy (UV-DRS), X-ray diffraction (XRD), Scanning electron microscopy (SEM), Energy dispersive x-ray analysis (EDAX), and High-resolution transmission electron microscopy (HRTEM) and selected area diffraction. This characterization confirmed the structure of $MgZrO_3$@Fe_2O_3@ZnO and also confirmed excellent photocatalytic activity for the decolorization of Nigrosin dye under ambient conditions. The 96±0.5 % degradation was observed within 60 min using 20 ppm Nigrosin dye solution with 0.2 g of $MgZrO_3$@Fe_2O_3@ZnO core-shell nanoparticles. A mechanistic approach for photodegradation of dye was established by Liquid chromatography-mass spectrometry (LCMS) with the identification of numerous smaller fragment molecule

Keywords: *Core-shell oxide, Photocatalytic degradation, Nigrosin dye, LC-MS analysis*

How to cite this article

Shelke Y. R., Bobade V. D., Tope D. R., Agashe J. A., Borhade A. V. Synthesis, Characterization and Photocatalytic Application of $MgZrO_3$@Fe_2O_3@ZnO Core-Shell Oxide for the Degradation Nigrosine Dye. J. Water Environ. Nanotechnol., 2022; 7(2): 155-169.

DOI: 10.22090/jwent.2022.02.004

INTRODUCTION

Environmental issues have become raised much worse in recent decades due to economic and industrial growth [1]. Large amounts of hazardous water containing harmful contaminants have been generated because of industrial and agricultural research. Organic dyes are amongst the most prominent kinds of pollutants found in the textile industry wastewater. Tint wastewater has a detrimental impact, including environmental contamination and genotoxicity from products [2]. Textiles, cosmetics, paper mills, plastic, leather industries, pharmaceuticals industries, and even food recently use chemically synthesized hues extensively [3-6]. The majority of them are azo dyes, such as methyl orange, Congo red, Rhodamine 6G, methylene blue, and others, which already have chromophores in their microstructures and therefore are pigmented. Spilling these chemicals into lakes, rivers, and groundwater during manufacturing, on either hand, represents an important public health risk hence dyes mutate into noxious, unpredictable, and cytotoxic components [7]. The discharge of large volumes of colorants into the ecosystem is a matter of social concern, legislative issues, and a significant challenge for scientific experts [8].

* Corresponding Author Email: *ashokborhade2007@yahoo.co.in*

For the treatment of these toxins, many chemical, physical, and biological procedures have already been used such as comprising reverse osmosis, chemical coagulation/flocculation, biological treatments, membrane filtering, and adsorption processes [9-13]. Apart from these approaches, nanomaterials and their related photocatalysts have shown potential in the removal of organic wastes. By illuminating the target wastewater with UV light, a range of semiconductor metal oxide nanoparticles, nanotubes, and nanoflowers have recently been employed as photocatalysts to degrade a variety of organic dyes [14 ,15].

In the present decade, nanomaterials have received great attention in the literature due to their various properties and applications in drug delivery, electronic devices, microwave devices, biosensors, catalysts, and photocatalysts. Metal oxides may take on a wide variety of structural geometries with an electronic structure that can display metallic, semiconductor, or insulator properties, and so play a critical role in a wide range of chemistry, physics, and materials science applications [16-20]. As a result, dyes are the most studied photocatalytic degradation substrates under solar light or UV light, compared with other natural compounds, because they are heavy industry pollutants [21]. TiO_2 [22], Ag nanoparticles [23], ZnO [24], Graphene-Ag/ZnO [25], and are some of the nano photocatalysts. Heterogeneous photocatalysis utilizing metal oxides has garnered a lot of attention in recent years because of its potential uses in both environmental and organic synthesis [26-30]. Semiconducting metal oxide nanoparticles absorb photons and produce electron-hole pairs, which may be utilized to oxidize or reduce materials on the photocatalyst surface. [31,32]. This feature has sparked a lot of interest in photocatalysts and their potential uses in domains like environment purification [33,34] and sustainable energy like water electrolysis. According to the review, the characteristics of these kinds of materials for purifying water are their durability, relatively low cost, and enhanced degradability [35]. Furthermore, the methodology eliminates the necessity for particle recovery after the treatment method [36].

In this study, we have synthesized the novel core-shell nanostructure $MgZrO_3@Fe_2O_3@ZnO$ photocatalyst for the degradation of Nigrosin dye [37-38]. The performance of $MgZrO_3$, $MgZrO_3@Fe_2O_3$, and $MgZrO_3@Fe_2O_3@ZnO$ nanostructure photocatalysts for mineralization of organic pollutants has been comprehensively proved in the current work, UV-DRS, XRD, FE-SEM, EDAX, and HR-TEM techniques were used to characterize the synthesized materials. The photocatalytic performance of $MgZrO_3@Fe_2O_3@ZnO$ was examined for the rapid decolorization of Nigrosin dye under UV-light exposure at room temperature. The catalyst was recycled five times and the structural stability of the recycled nanomaterial was confirmed. The degradation performance of Nigrosin dye was analyzed using UV-VIS and the mechanism of photodegradation was confirmed by liquid chromatography-mass spectrometry. The impact of a double Fe_2O_3 and ZnO coating on the $MgZrO_3$ photocatalyst was investigated in detail.

EXPERIMENTAL

Reagents and materials

Commercially available Magnesium chloride ($MgCl_2$, Merck, 99.00%), Zirconium oxychloride ($ZrOCl_2$, Merck, 99.90%), Ferric nitrate ($Fe(NO_3)_3$ Merck, 99.50%), Zinc chloride ($ZnCl_2$, Merck, 99.90%), Triton-X-100 (Loba, 98.00%), Sodium chloride (NaCl, Loba, 99.00%), Sodium sulphate (Na_2SO_4, Loba, 98.00%), Sodium carbonate ($Na_2(CO_3)$, Loba, 99.50%), Sodium nitrate ($NaNO_3$, Loba, 99.90%), Ethylenediamine tetraacetic acid (EDTA, Sigma Aldrich, 99.00 %) Isopropyl alcohol (IPA, Merck, 99.00%) and Nigrosin dye (NI, Sigma Aldrich, 99.00 %), with an analytical grade were purchased and used without further purification. The stock (100 ml) solution of Nigrosin dye was prepared using deionized water. The experimental solution of the chosen concentration of Nigrosin dye (5, 10, 15 20, and 25 mg/L) was prepared by further dilution of the stock solution with deionized water.

Preparation of Magnesium (II) zirconate nanoparticles

The nanoparticle of $MgZrO_3$ was synthesized by the sol-gel method. The Magnesium chloride [$MgCl_2$] (1 M) and Zirconium oxychloride [$ZrOCl_2$] (1 M) was taken in a Teflon autoclave and dissolved using 100 mL of double-distilled water, Triton X-100 was added in the above solution. To obtain a precipitate solution with a pH of 9-10, a 2 M NaOH solution was gently added under vigorous stirring. The steel-lined Teflon autoclave was kept in an oven at 120 °C for 24 h. The resulting gel was filtered and rinsed with distilled water multiple times. The washed precipitate was then dried at 110 °C for 6 h and then calcined at 800 °C for 6 h to remove the surfactant.

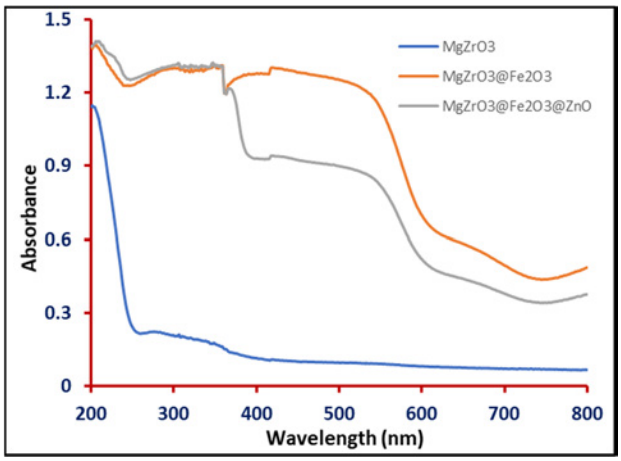

Fig.1. UV-DRS analysis of modified $MgZrO_3$ photocatalyst.

Preparation of $MgZrO_3$@Fe_2O_3 core-shell nanoparticles

The Fe_2O_3 coating on magnesium (II) zirconate was carried out by mixing $MgZrO_3$ (1 M) and Ferric nitrate $Fe(NO_3)_3$ (2 M) with the appropriate addition of Triton X-100 as a surfactant in 100 ml double distilled water. To achieve the precipitate, a further NaOH solution (1 M) was added dropwise under vigorous stirring for 1 h. The resulting slurry was kept in an oven at 120 °C for 24 h. To remove the organic materials, the precipitate was washed with distilled water and dried at 110 °C for 4 h before being calcined at 650 °C for 6 h. TEM studies validated the coating layer of Fe_2O_3.

Preparation of $MgZrO_3$@Fe_2O_3@ZnO core-shell nanoparticles

The $MgZrO_3$@Fe_2O_3@ZnO core-shell nanoparticles were prepared by mixing $MgZrO_3$@Fe_2O_3 (1.1 M), Zinc chloride ($ZnCl_2$) (1.2 M), and a known amount of Triton X-100 into 100 ml NaOH (2 M) solution under vigorous stirring for 2 h and kept into steel-lined Teflon autoclave in an oven at 120 °C for 24 h. When the reaction was completed, the precipitate obtained was filtered and cleaned with deionized water and dried at 120 °C for 4 h. The dried product was ground in mortar-pestle to prepare fine powder. The gained powder was smashed and afterward calcined at 700 °C for 6 h to obtain a polycrystalline powder. The two layers of coating on $MgZrO_3$ are authenticated by TEM analysis.

Material characterization

A variety of analytical methods were used to characterize the materials. The optical and band gap energy was studied by using UV-DRS analysis which is confirmed on UV-DRS Shimadzu-2400 Instrument. An XRD analysis of the samples was carried out using a copper X-ray diffractometer operated at 40 kV and 40 mA with a scanning rate of 1°/minute. The morphology of the samples was analyzed using FE-SEM and TEM. A NOVA NANOSEM NPEP303 electron microscope equipped with a 15 kV accelerating voltage instrument was used for the FE-SEM study, and energy-dispersive X-ray analysis techniques (EDAX) were used in conjunction with the same instrument to determine elemental compositions. The crystallinity of magnesium (II) zirconate and core-shell nanostructures were determined using a transmission electron microscope (HRTEM-JEOL/JEM 2100, operating voltages 200 kV, LaB6 Electron gun, point resolution 0.23 nm, Lattice resolution 0.14 nm).

photocatalytic degradation experiments

The photocatalytic activity of the $MgZrO_3$@Fe_2O_3@ZnO heterocatalyst was evaluated using the degradation of a Nigrosin dye aqueous solution exposed to visible light irradiation. A reaction mixture of dye ($\approx 10^{-5}$ M) and 0.2 g photocatalyst was irradiated with a 20W UV lamp (Philips) in a photoreactor. The progress of the dye degradation was monitored by measuring the absorbance of the reaction mixture at regular time intervals using a UV-Vis spectrophotometer (Systronics, India) at 576 nm. It was observed that the absorbance of the dye solution decreases with the increasing time of exposure, which indicates that the concentration of Nigrosin dye decreases.

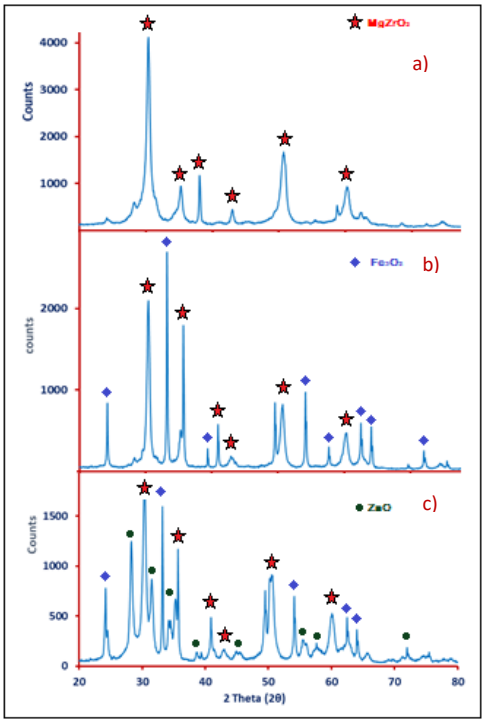

Fig. 2. XRD analysis of a) $MgZrO_3$, b) $MgZrO_3@Fe_2O_3$ and c) $MgZrO_3@Fe_2O_3@ZnO$

RESULTS AND DISCUSSION

Optical Studies of the $MgZrO_3@Fe_2O_3@ZnO$ Nanoparticles

The spectra of $MgZrO_3$ core-shell nanocrystals for ultraviolet light are shown in Fig. 1. In nanocomposites, the band gap is determined by crystallite size, shape, and structural imperfections [39]. Fig.1 gives the absorption peaks at 260 nm, 410 nm, and 432 nm for $MgZrO_3$, $MgZrO_3@Fe_2O_3$, and $MgZrO_3@Fe_2O_3@ZnO$ core-shell nanoparticles respectively. Both of the core-shell nanocrystals demonstrated high absorption spectra between 410 and 432 nm. As a result of this hypsochromic variation in absorption, the band gap energies of both materials were affected. The band gap energies were calculated by Eg (eV) = 1240/(wavelength in nm) using absorption peaks and found 4.96 eV for $MgZrO_3$, 3.14 eV for $MgZrO_3@Fe_2O_3$ core-shell nanoparticles, and 2.98 eV for $MgZrO_3@Fe_2O_3@$ ZnO core-shell nanoparticles.

X-ray diffraction patterns (XRD)

The X-ray diffraction pattern of magnesium zirconate is shown in Fig. 2(a). The pattern indicated a dominant cubic zirconia phase with a small contribution of cubic magnesium oxide, the structure is in good agreement with the standard JCPDS card No. 27-997 and 1-1235 respectively. No other impurity peaks were visualized in the XRD, this indicates good purity of the prepared material. In Fig.2 (b) the presence of Fe_2O_3 with $MgZrO_3$ and the crystalline nature of hematite (α-Fe_2O_3) were confirmed by XRD. XRD patterns showed the different reflection peaks with respect to corresponding lattice planes which is matched with JCPDS no.89-1165. The diffraction planes such as (012), (104), (110), (113), (024), (116), (122), (214), and (300) were noticed in the irrespective diffraction angles 26.23°, 36.50°, 42.86°, 56.24°, 64.90° and 74.00° respectively, no other peak from impurities were noticed in the XRD spectra.

Figure 2(c) illustrates the existence of Fe_2O_3 and ZnO phases in $MgZrO_3@Fe_2O_3@ZnO$ core-shell nanoparticles, indicating that ZnO was coated on the Fe_2O_3 nanoparticles. The 2θ values with reflection planes at 28.25° (100), 34.39° (002), 36.23° (101), 47.44° (102), 54.34° (101) and 56.78° (200) corresponds to JCPDS Card No. 36-1451. So, all diffraction peaks fit well with the hexagonal wurtzite structure of ZnO. The particle size of core-shell nanoparticles was calculated by using Scherer's formula [40], which gives 32.25,

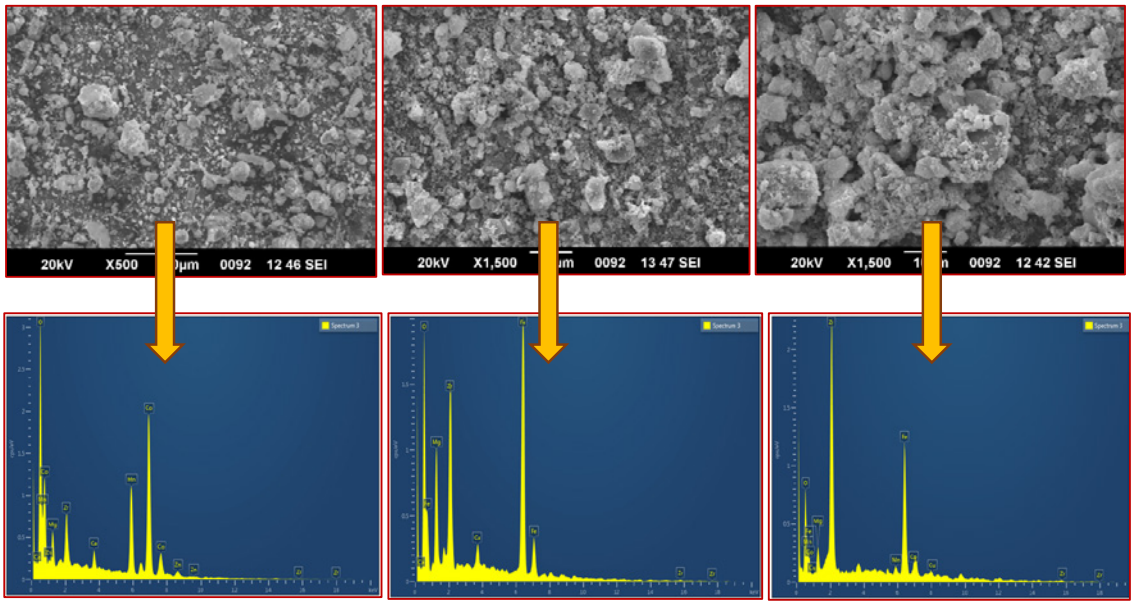

a) b) c)

Fig. 3. SEM and EDAX analysis of a) $MgZrO_3$ b) $MgZrO_3@Fe_2O_3$ c) $MgZrO_3@Fe_2O_3@ZnO$.

41.74, and 34.25 nm for $MgZrO_3$, $MgZrO_3@Fe_2O_3$, $MgZrO_3@Fe_2O_3@ZnO$ nanocrystals respectively.

Scanning electron microscope (SEM) analysis

The structural morphology of nanoparticles was studied and analyzed using SEM, and it gives significant information regarding the size, shape, and growth mechanism as shown in Fig. 3(a-c). The SEM imaging of magnesium zirconate particles generated by the sol-gel method is shown in Fig. 3(a). The finding of spherical morphologies with the crystal habit minerals is supported by XRD data [41]. Fig. 3(b) SEM analysis of the surface morphology and distribution of $MgZrO_3@Fe_2O_3$ crystals reveals that multi-dimensional nanoparticles with spherical shapes were formed. Fig. 3(c) shows typical SEM images of $MgZrO_3@Fe_2O_3@ZnO$, which reveal the sample's anatomy, which is susceptible to aggregation due to the spherical and granular surface area to volume ratio at both resolutions.

The aggregation of particles occurs as a result of nanoparticles with an uneven spherical form grown to a bigger size with well-delineated limits. The surface-to-volume ratio of these spherical-shaped nanoparticles is high, giving for a large number of active sites. These sites promote the photocatalytic capacity of nanomaterials by absorbing UV light and forming an electron-hole pair and they are also dependent on grains inside interconnections.

EDAX spectroscopy was used to analyze the distribution and chemical composition of the $MgZrO_3@Fe_2O_3@ZnO$ core shell. The result of the EDAX analysis confirms the presence of Mg, Zr, O, Fe, and Zn elements in the prepared core-shell sample and is confirmed by the elemental peaks attributable to these elements in the inserted EDAX spectrum without other impure peaks.

In the EDAX spectrum, Fig. 3(a) shows strong peaks for magnesium at 1.2 keV and zirconate at 2.2, and 0.2 keV, while the iron is present at 6.5 keV in coated magnesium zirconate with Fe_2O_3, which is depicted in Fig. 3(b) on the same scale as magnesium and zirconate. In Fig. 3(c) the elemental analysis of $MgZrO_3@Fe_2O_3$ coated with zinc oxide shows a significant peak at 8.5 keV due to Zn.

Transmission electron microscopy (TEM) analysis

The surface shape and particle size of the obtained $MgZrO_3@Fe_2O_3@ZnO$ nanocrystals are shown in the TEM picture in Fig. 4(c). The image shows that $MgZrO_3@Fe_2O_3@ZnO$ powder is made up of nanometric particles with nanocrystal sizes of 20-40 nm. It was impossible to examine the particles separately since they overlapped. The morphology was validated by TEM which revealed

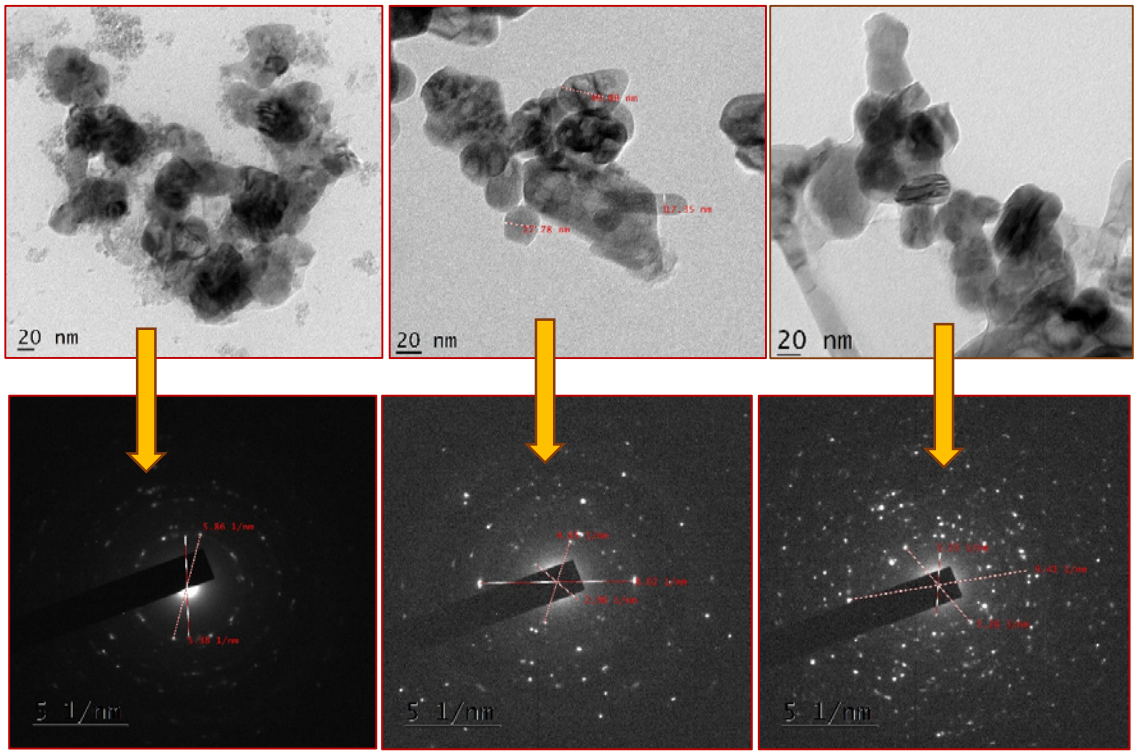

Fig. 4. TEM and SAED analysis of a) $MgZrO_3$ b) $MgZrO_3$@Fe_2O_3 c) $MgZrO_3$@Fe_2O_3@ZnO.

a spherical shape and varied-sized agglomerates made up of smaller particles in the $MgZrO_3$@Fe_2O_3@ZnO core-shell. This might be the result of tiny particles coalescing into agglomerates. Fig. 4 shows an analysis of periodic lattice fringes in a high-resolution transmission electron microscopy (HRTEM) picture.

The primary coating layer surrounds the core with Fe_2O_3 with ZnO seated on top of the Fe_2O_3 as the secondary coating layer. The homogeneous coating of Fe_2O_3 and ZnO on $MgZrO_3$ is due to complete layer matching between Fe_2O_3 and ZnO. In Fig. 4(c), two types of coatings are visible on the $MgZrO_3$ nanoparticles that are the subject of the dual-coated $MgZrO_3$ sample.

Photocatalytic Degradation of Nigrosin dye

The obtained $MgZrO_3$@Fe_2O_3@ZnO nanoparticles were exploited as an effective photocatalyst for degradation of the Nigrosin dye as a chosen pollutant. To choose the best condition for dye degradation, the different parameters were used such as the effect of dark and visible light irradiation, photocatalyst dosage, initial dye concentration, and irradiation time. A photocatalytic procedure was performed in a UV-transparent glass tube reactor with the absorbance being measured every 10 minutes using a spectrophotometer. Irradiating a dye solution (20 mg/L) with visible light has no effect on absorbance in the absence of a photocatalyst, as illustrated in Fig. 5. There were no changes in the dye degradation when 0.1 g $MgZrO_3$@Fe_2O_3@ZnO was added to the Nigrosin dye solution (20 mg/L) in the absence of light sources for 80 minutes. This result indicates that there was no dye adsorption on the catalyst. As a result, $MgZrO_3$@Fe_2O_3@ZnO alone has no deterioration.

Without light illumination, no Nigrosin dye degradation occurs in the presence of a catalyst, illustrating the necessity of light illumination [42]. The effect of visible light on the photolysis degradation of Nigrosin dye was investigated, and the dye concentration was found to be reduced when the dye was exposed to an aqueous solution. This work shows that light irradiation with only 0.1

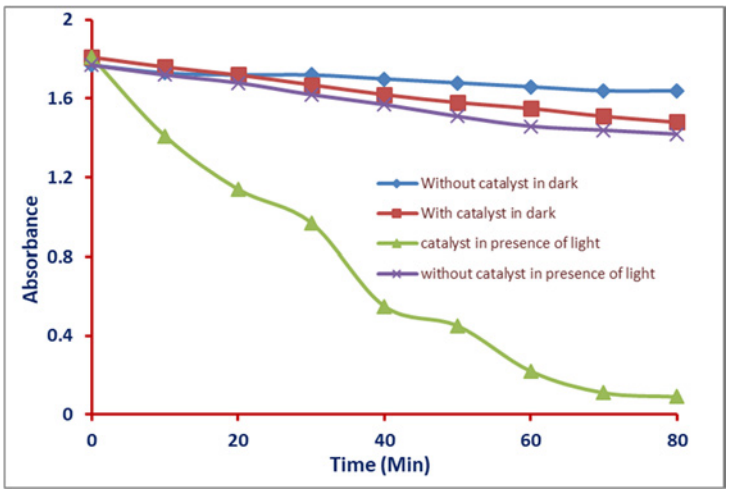

Fig. 5. Effect of catalyst and light irradiation on dye degradation.

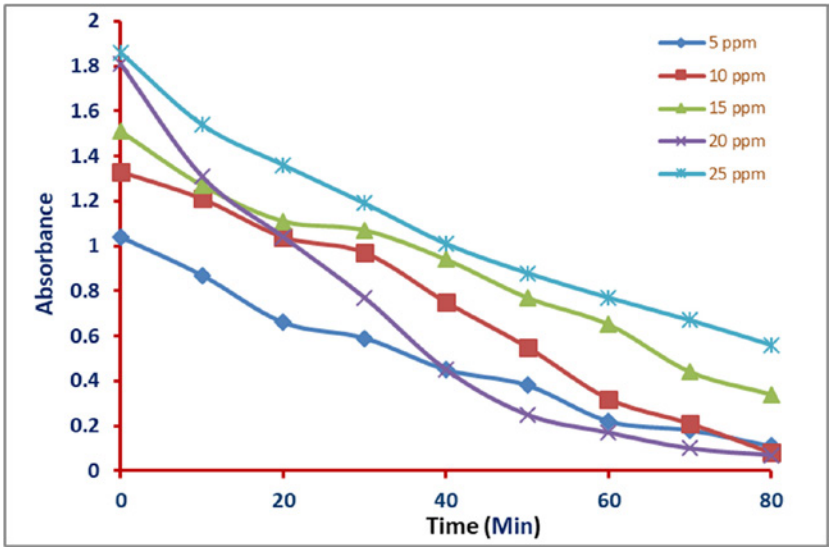

Fig. 6. Effect of initial dye concentration on the photocatalyst degradation of Nigrosine by using $MgZrO_3$@ Fe_2O_3@ZnO nanoparticles.

g of $MgZrO_3$@ Fe_2O_3@ZnO strengthened catalytic performance for both discoloration and breakdown of Nigrosin dye.

Effect of concentration of dye

The dye degradation is the prime factor that can affect the dye degradation efficiency. The influence of dye concentration on the rate of photocatalytic degradation was investigated utilizing produced magnesium zirconate, $MgZrO_3$@Fe_2O_3, and $MgZrO_3$@Fe_2O_3@ZnO core-shell nanoparticles with varying preliminary concentrations of Nigrosin dye (5,10,15,20 and 25 mg/L).

$MgZrO_3$@Fe_2O_3@ZnO core-shell nanoparticles exhibited improved 94 percent degradation of Nigrosin (20 mg/L) in 60 minutes, $MgZrO_3$@ Fe_2O_3 degradation in 80 minutes, and $MgZrO_3$ degradation in 80 minutes when the light was switched on for the appropriate period.

Under the light, $MgZrO_3$@ Fe_2O_3@ZnO allows the color of Nigrosin to fade over time. This is attributed to the appropriate band location and increased surface area as a result of the unique shape. This is due to the success of consolidating Fe_2O_3 and ZnO onto the $MgZrO_3$ spinel, which resulted in improved structural, morphological, and optical characteristics. The photocatalytic degradation adequacy of $MgZrO_3$@Fe_2O_3@ZnO

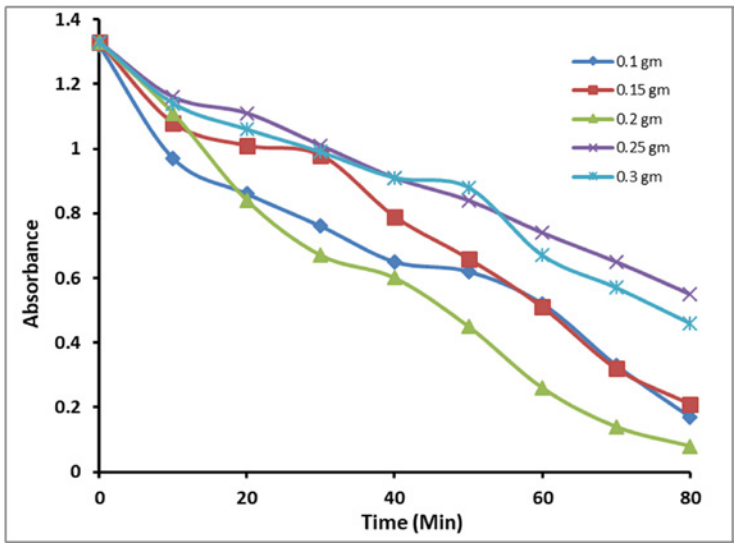

Fig. 7. Effect of amount of photocatalyst on nigrosine dye degradation.

decreased as the starting concentration of Nigrosin dye grew.

Effect of amount of catalyst

The impact of varying the quantity of catalyst on the rate of dye degradation has been seen over a wide range (0.1-0.5 g) while maintaining all other parameters constant. The degradation rate rises as the concentration of Photocatalyst increases, with $MgZrO_3$@ Fe_2O_3@ZnO core-shell reaching 0.2 g. With an increase in catalyst quantity above this limit, the rate of reaction becomes almost constant. The quantity of magnesium zirconate core-shell nanoparticles (0.1-0.5 g) in the presence of UV - visible light with Nigrosin dye (20 mM/L) solution is shown in Fig. 7.

As the catalyst concentration rises, the degradation rate lowered. The light scattering of the catalyst achieved this outcome. The photo-activated suspension volume was lowered when light penetrated the dye solution as the catalyst dosage was increased [43]. Some areas of the catalyst surface were found to be unresponsive to photon and dye absorption in this condition [44].

To evaluate the optical time of photodegradation, a series of tests were performed at a variant time and the results are given in Fig. 8. The λ_{max} of the chosen dye is located at 576 nm. It can be seen that 96 % of the dye degraded within 60 min. In this study, 0.2 g of $MgZrO_3$@ Fe_2O_3@ZnO core-shell nanomaterials per 100 ml of 20 mM/L Nigrosin dye solution was said to be the least addition. The degradation of dye before and after exposure to visible light and photocatalyst is depicted in Fig. 8. As the irradiation duration lengthens, the chromophoric absorption peak at 576 nm completely reduces the dark purple colorization of the Nigrosin dye solution. The color of the solution (absorbance 576 nm) changed considerably, indicating that in the presence of $MgZrO_3$@Fe_2O_3@ZnO core-shell nanoparticles, the absorbance falls to a minimum within 60 minutes.

Photodegradation mechanism

Advanced oxidation processes (APO) include photocatalytic pollution clean-up, which has shown to be a difficult technique for organic compounds. Because semiconductors are inexpensive and can easily mineralize diverse organic contaminants, this approach is more suited and efficient than other APOs. The photocatalytic discoloration of Nigrosin dye occurs as a result of the following events.

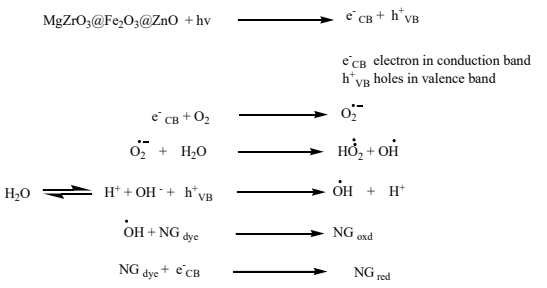

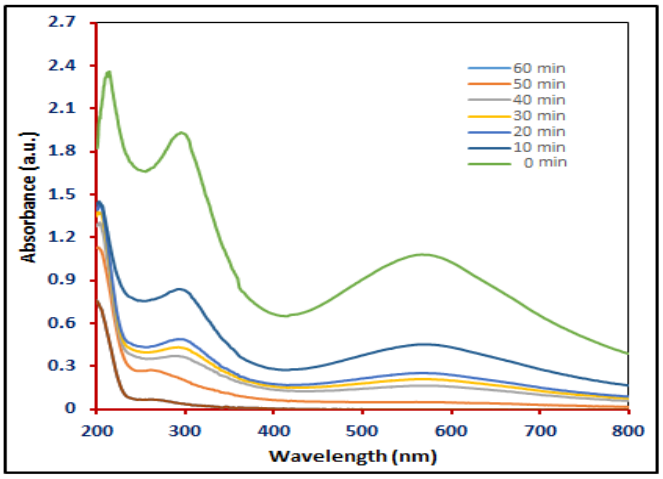

Fig. 8. Degradation of Nigrosine dye before and after exposure to visible light and photocatalyst with time.

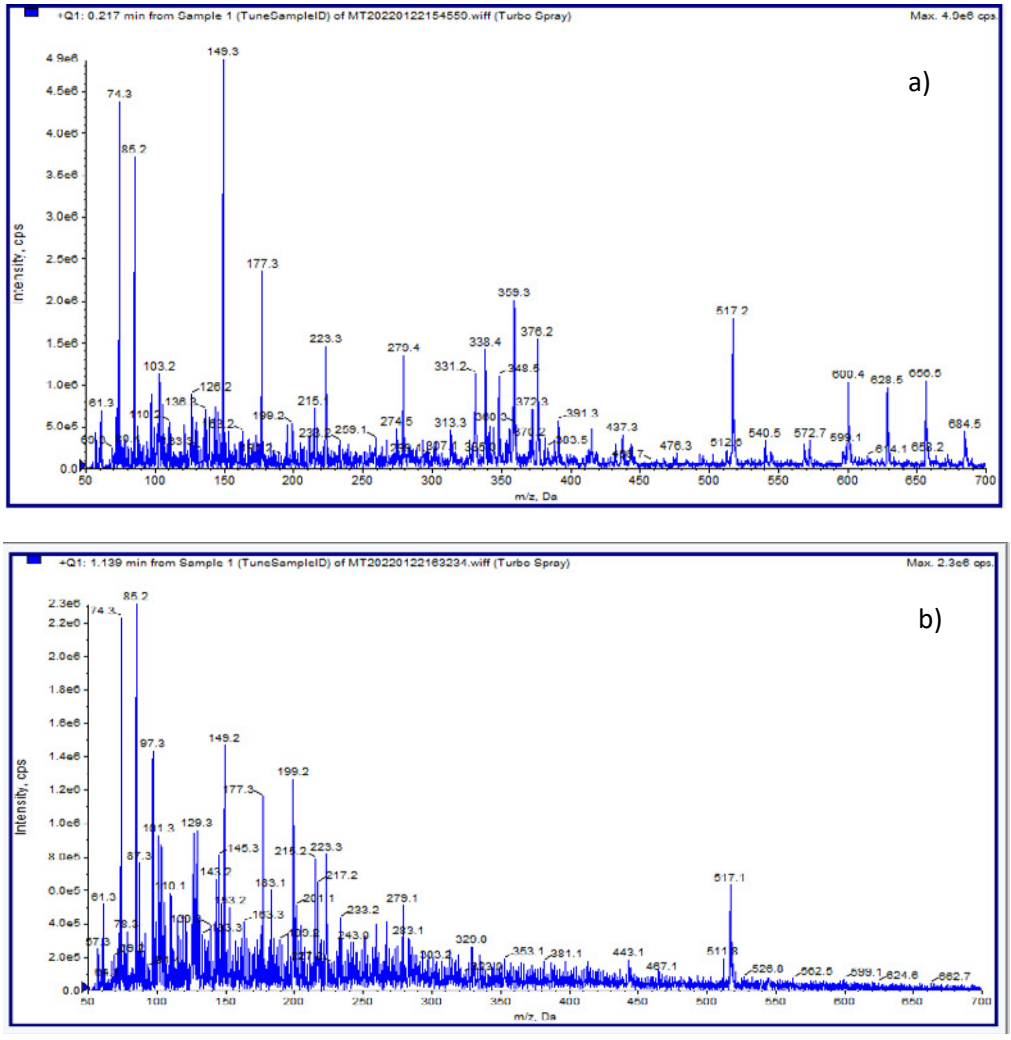

Fig. 9. LC-MS analysis of Nigrosine dye a) before and b) after degradation.

This process prevents the recombination of electrons and holes. The radicals formed in the foregoing processes, ·OH and $\cdot O_2$, can then react with the Nigrosin dye to make additional species, which is the direct cause of the dye's discoloration.

LC-MS analysis of the Nigrosin dye breakdown pathway

To illustrate the degradation pathway and establish the degradation of colorless species, a qualitative evaluation was carried out using Liquid Chromatography-Mass Spectrometry (LC-MS). Under UV-visible irradiation, the mass spectrum of Nigrosin dye solution before photodegradation by $MgZrO_3$@Fe_2O_3@ZnO core-shell nanoparticles is presented in Fig. 9(a). The decrease in m/z of Nigrosin dye revealed fragmentation products is depicted in Fig. 9(b). The structure of various products was postulated using HPLC-MS fragmentation. The m/z 512, 363, 159, 151, 143, 127, 123, 77, and 54 fragments showed excellent degradation of a large Nigrosin dye molecule with a molecular weight of 616. The possible mechanism of degradation of Nigrosin dye was given in Fig. 10.

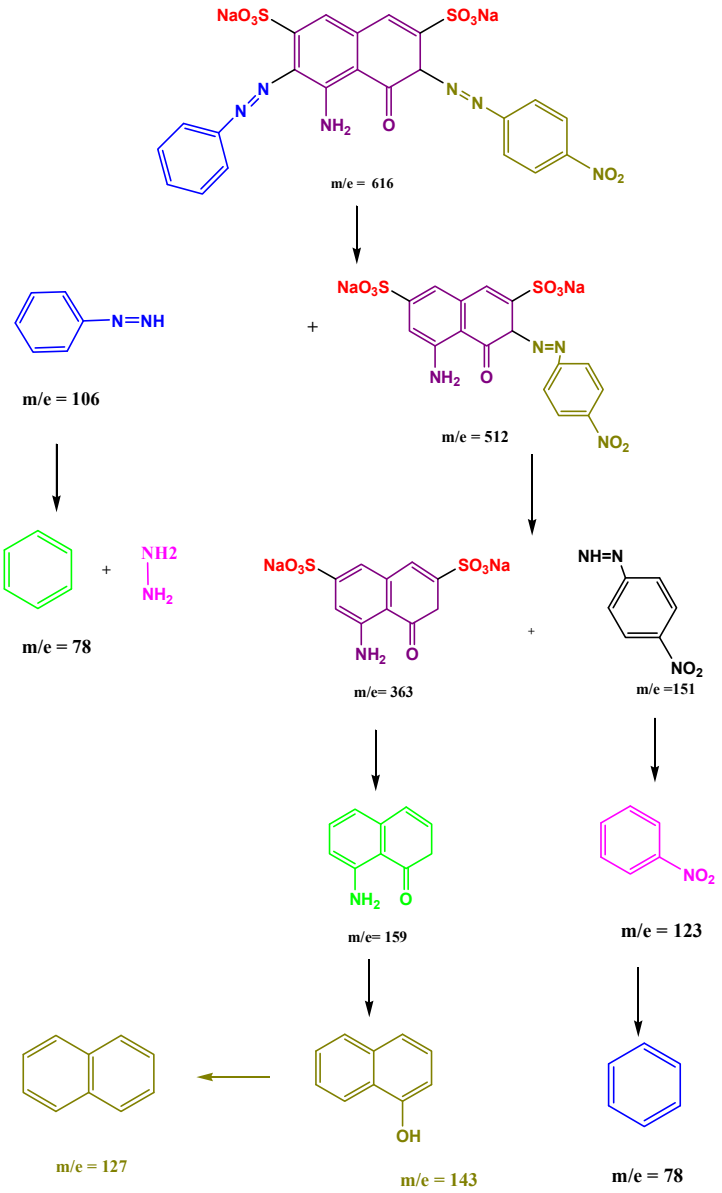

Fig. 10. Degradation mechanism of Nigrosine dye

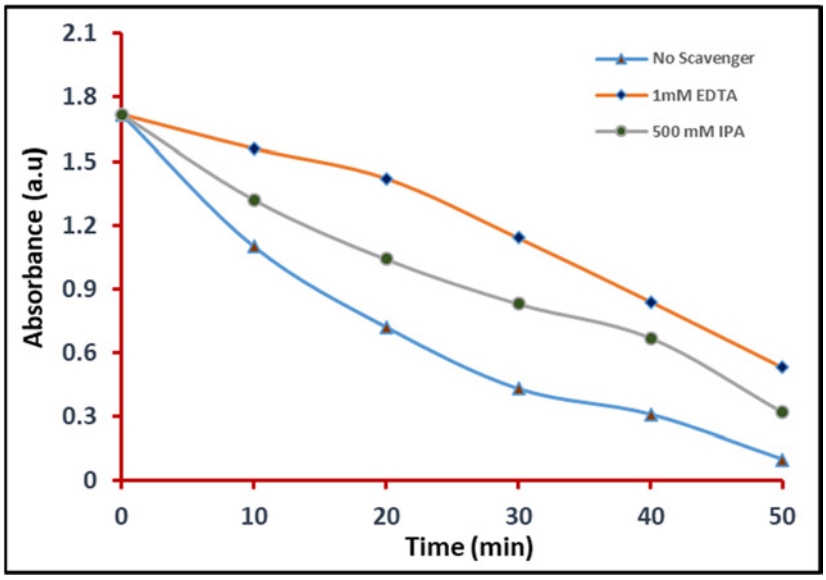

Fig. 11. Scavenger experiment for photocatalytic degradation of Nigrosine dye by using $MgZrO_3$@Fe_2O_3@ZnO catalyst.

Detection of active species by scavenger experiment

The use of scavengers to trap holes and free electrons is a beneficial method for elucidating the process of organic pollutant photocatalysis. Fig. 11 shows the photocatalytic activity of magnesium zirconate core-shell nanoparticles for Nigrosin dye.

The OH active species were captured using EDTA, whereas the O_2 active species were trapped with isopropyl alcohol [45]. During the scavenger experiment, it was discovered that a very little amount of EDTA hindered the breakdown process. As a deactivator of OH active species, EDTA shows that the most common active species involved in photocatalytic degradation were OH, which is produced by the absorption of UV-Visible light and forms a large number of holes.

Furthermore, EDTA molecules can interact with the surface of the catalyst to restrict dye molecule interaction, which is necessary for photodegradation, demonstrating the importance of surface interaction. Furthermore, adding IPA (Isopropyl alcohol) to magnesium zirconate and core-shell nanoparticles lowered their catalytic efficacy somewhat, supporting the little role of O_2 radicals in the destruction of both organic molecules. As a consequence, the capturing experiment confirmed the OH's predominance in Nigrosin dye degradation [46].

The effect of salinity

When salts are added, the salting-out effect may affect the removal efficiency. In the presence of 0.5 gm NaCl, Na_2SO_4, $Na_2(CO_3)$, and $NaNO_3$ aqueous solutions, the influence of salt on removal efficiency was investigated. In the addition of inorganic salts, the dye removal efficiency of $MgZrO_3$@Fe_2O_3@ZnO rises, as seen in Fig.12. This demonstrates that dye adsorption on $MgZrO_3$@Fe_2O_3@ZnO is aided by the presence of salt. The salting-out idea may be used to explain how salt can help with adsorption [47,48] The solubility of the dye in water is increasingly restricted as the number of salt increases. The salting-out effect reduces the dye's solubility, causing more dye molecules to diffuse to the surface of $MgZrO_3$@Fe_2O_3@ZnO and increasing adsorption efficiency. As a result, the highest Nigrosin dye elimination was obtained in the presence of $NaNO_3$ salt.

Kinetic study

In Fig. 13, when the absorbance data of Nigrosin dye are plotted in ln(Ao/A) versus time dependant normalized dye concentrations (which is the ratio between the initial concentration and the concentration upon reaction), a linear plot is obtained. This indicates that the decomposition of Nigrosin dye follows first-order kinetics. The rate constant of $MgZrO_3$@Fe_2O_3@ZnO core-shell nanoparticles is 0.06329 min^{-1}.

Chemical Oxygen Demand (COD)

The mineralization of nigrosin dye was

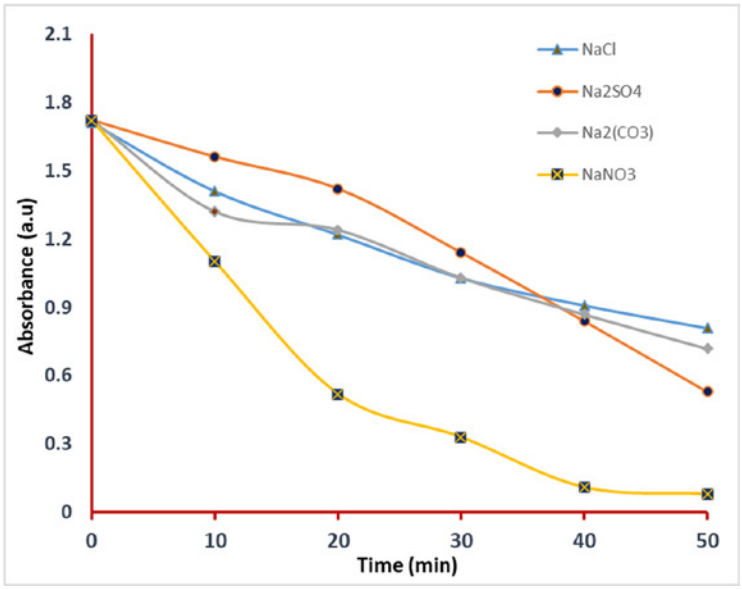

Fig. 12. Effect of salinity on photocatalytic degradation of Nigrosine dye by using $MgZrO_3$@Fe_2O_3@ZnO catalyst.

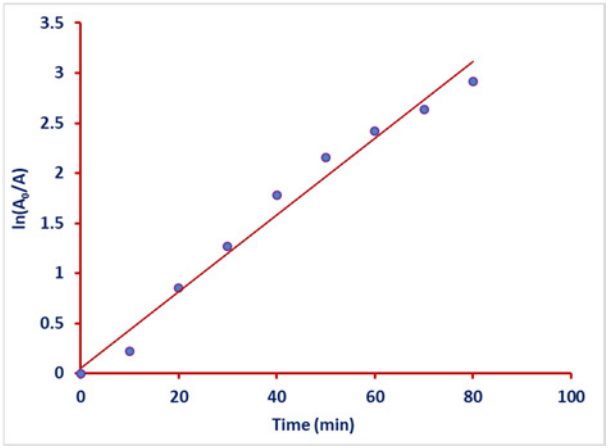

Fig. 13. Kinetic study on Nigrosin dye degradation using $MgZrO_3$@Fe_2O_3@ZnO nanoparticles

confirmed by measuring the decrease in COD value. COD of nigrosin dye solution was estimated before and after the photocatalytic treatment and the photodegradation efficiency of the catalyst was calculated using the following equation:

$$\%.\ \eta = \frac{COD_{before} - COD_{after}}{COD_{before}} \text{ x } 100$$

% η = Photodegradation efficiency (%), COD before = COD of dye solution before exposure of light and CODafter = COD of dye solution after exposure of light COD of dye solution before and after exposure of light has been determined by the redox method. The photodegradation efficiency after 60 min of exposure to light on Nigrosin dye using $MgZrO_3$@Fe_2O_3@ZnO nanoparticles was found to be 96.08. The COD of dye solution before dye degradation was found 71.34 mg/l whereas after dye degradation it was decreased up to 2.79 mg/l.

Recyclability study

For each catalytic process, the catalyst's stability and recyclability are more crucial. After the process, the $MgZrO_3$@Fe_2O_3@ZnO core-shell nanostructure catalyst was recovered and its recyclability for dye

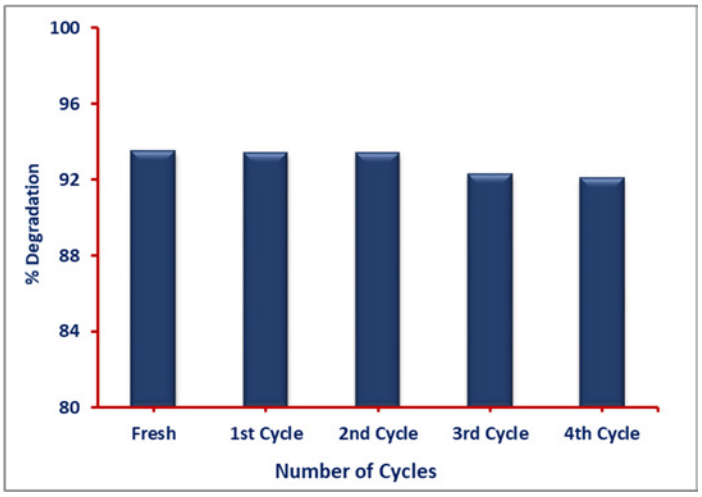

Fig. 14. Recyclability study for photocatalytic degradation of Nigrosine dye.

Table. 1. Comparative study of catalysts for degradation of Nigrosin dye.

Sr. No.	Catalyst	Degradation time and (%)	Catalyst Loading	TON	Reference
1	$La_2Ce_2O_7$	2 hrs (78.87%)	0.8	98.58	50
2	TiO_2	60 min (89 %)	0.5	178	51
3	$FeSO_4.7H_2O$	2 hrs (78 %)	0.5	156	52
4	$MgZrO_3$	80 min (76 %)	0.2	380	Present work
5	$MgZrO_3@Fe_2O_3$	80 min (81 %)	0.2	405	Present work
6	$MgZrO_3@Fe_2O_3@ZnO$	60 min (96 %)	0.2	470	Present work

degradation was investigated. For the recyclability investigation, the same degrading technique was used.

The produced $MgZrO_3@Fe_2O_3@ZnO$ core-shell nanostructure catalyst was photo catalytically reusable for three cycles, with a slight decline in efficacy until the fourth cycle, when the percent degradation reduces drastically, as shown in Fig. 14. This might be due to a loss of catalyst and a reduction in active sites on the catalytic surface throughout the recovery process.

Comparison of the results

Table 2 compares Nigrosin dye catalytic performance with other photocatalysts described in the literature. This shows that photocatalysts are mentioned in a modest number of papers. Moreover, the current work is the first of its sort to report the clearance of Nigrosin dye with novel core-shell nanoparticles. In comparison to Table 1, the photocatalytic degradation performance of the $MgZrO_3@Fe_2O_3@ZnO$ core-shell nanoparticles was considerably greater in a shorter time. In comparison to the mentioned papers, this shows that $MgZrO_3@Fe_2O_3@ZnO$ core-shell nanoparticles are a suitable choice and an alternative to traditional photocatalysts. The turnover number (TON) has been calculated by using this formula [49].

CONCLUSION

$MgZrO_3@Fe_2O_3@ZnO$ core-shell nanoparticles were effectively synthesized using the sol-gel method and then employed for UV light-driven photocatalysis of Nigrosin dye. $MgZrO_3$ was effectively stabilized in an aqueous solution by a double covering of Fe_2O_3 and ZnO, which also exhibited its oxidation. The developed catalyst showed enhanced photocatalytic efficiency at the lowest catalyst dosage. The catalyst was very efficient for several cycles, with the increased formation and low recombine frequencies of electron-hole pairs; consequently, it may be employed as an appropriate photocatalyst for dye pollutant treatment from polluted water. Furthermore, the $MgZrO_3@Fe_2O_3@$ ZnO core-shell nanoparticles can be used four times without losing their degrading activity, and the catalyst can be easily extracted via filtering. The photocatalytic material was also steady, according

to the reusability tests. This study might lead to the development of a dye wastewater treatment technology.

DECLARATION OF CONFLICTS INTEREST

The authors state that they have no known competing financial interests or personal ties that might have influenced the research presented in this study.

REFERENCES

[1] Hashimoto K, Irieand H, Fujishima A (2005) TiO_2 photocatalysis: a historical overview and future prospects. Jpn. J. Appl. Phys. 44;8269.

[2] Salvi N, Banu R, Ameta C, Punjabi PB (2021) Enhanced photocatalytic degradation of Nigrosin dye from its aqueous solution using $La_2Ce_2O_7$ nanoparticles. Ind. J. Chem. Technol. 28;172-179.

[3] Mohammed TJ (2017) UV-a activated ZnO mediated photocatalytic decolorization of Nigrosin (acid black 2) dye in aqueous solution. J. Geosci. Environ. Protect. 5;138-147

[4] Teh CY, Budiman PM, Shak KPY, Wu TY (2016) Recent advancement of coagulation–flocculation and its application in wastewater treatment. Ind. Eng. Chem. Res. 55;4363.

[5] Chen X, Wu Z, Liu D, Gao Z (2017) Preparation of ZnO photocatalyst for the efficient and rapid photocatalytic degradation of azo dyes. Nanoscale Res. Lett. 12;143.

[6] Franciscon E, Grossman MJ, Paschoal JA, Reyes FG and Durrant LR (2019) Efficient dye decolorization of an azo dye on fish scale hydroxyapatite. Res. J. Pharm. Technol. 12; 2917.

[7] Natarajan S, Bajaj HC and Tayade RJ (2018) Recent advances based on the synergetic effect of adsorption for removal of dyes from waste water using photocatalytic process. J. Environ. Sci. 65;201-222.

[8] Esther F, Tibor C, Gyula O (2004) Removal of synthetic dyes from wastewaters: a review. Environ Int. 30;953-971

[09] Hamedi A, Zarandi M.B and Nateghi M.R(2019) Highly efficient removal of dye pollutants by MIL-101(Fe) metal-organic framework loaded magnetic particles mediated by Poly L-Dopa. J. Environ. Chem. Eng. 7;102882.

[10] Hitkari G, Singh S and Pandey G, (2017) Synthesis, characterization and visible light degradation of organic dye by chemically synthesized ZnO/γ-Fe_2O_3 nanocomposites. Int. Adv. Res. J. Sci. Eng. Technol. 4;3960–3965.

[11] Fu K, Huang J,Yao N, Xu X, and Wei M (2015) Enhanced photocatalytic activity of TiO_2 nanorod arrays decorated with cdse using an upconversion TiO_2:Yb^{3+},Er^{3+} thin film. Ind. Eng. Chem. Res. 54;659-665.

[12] Bhatia D, Sharma N.R, J. Singh and Kanwar R.S (2017) Biological methods for textile dye removal from wastewater: A review. Crit. Rev. Environ. Sci. Technol. 47;1836–1876.

[13] Seow T.W, and Lim C. K, (2016) Removal of dye by adsorption: A review. Int. J. Appl. Bioeng 11;2675–2679.

[14] Kiwaan H.A, Atwee T.M, El-Bindary A.A (2020) Photocatalytic degradation of organic dyes in the presence of nanostructured titanium dioxide. J. Mol. Struct. 1200;127-115.

[15] Velusamy P, Pitchaimuthu S, Kannan N (2014) Modification of the photocatalytic activity of TiO_2 by b-cyclodextrin in decolouration of ethyl violet. J. Adv. Res. 5;19–25.

[16] Cao J, Zhu Y, Shi L, Zhu L, Bao K, Liu S, Qian Y (2010) Double-shelled Mn_2O_3 hollow spheres and their application in water treatment. Eur. J. Inorg. Chem. 1172.

[17] Zhao J, Tao Z, Liang J, Chen J (2008) Facile Synthesis of nanoporous γ-MnO_2 structures and their application in rechargeable Li-ion batteries. Cryst. Growth Des. 8;2799.

[18] Moon T, Yu J, Park J, Park YI, Na HB, Kim BH, Song IC, Moon WK, Hyeon T (2009) Various-shaped uniform Mn_3O_4 nanocrystals synthesized at low temperature in air atmosphere. Chem. Mater. 21;2272.

[19] Ding Y, Hou C, Li B, Lei Y (2011) Preparation of TiO_2–Pt hybrid nanofibers and their application for sensitive hydrazine detection. Electroanalysis. 23;1245.

[20] Amini M, Naslhajian H, Farnia SMF (2014) V-doped titanium mixed oxides as efficient catalysts for oxidation of alcohols and olefins. New J. Chem. 38;1581

[21] Yola ML, Eren T, Atar N, Wang S (2014) Adsorptive and photocatalytic removal of reactive dyes by silver nanoparticle-colemanite ore waste. Chem. Eng. J. 242;333–340.

[22] Ahmad M, Ahmed E, Hong Z.L, Khalid N.R, Ahmed W, Elhissi A (2013) Graphene-Ag/ZnO nanocomposites as a high performance photocatalyst under visible light irradiation. J. Alloys Compd. 577;717–727.

[23] Velmurugan R, Swaminathan M (2011) An efficient nanostructured ZnO for dye sensitized degradation of reactive red 120 dye under solar light, Sol. Energy Mater. Sol. Cells. 95;942–950.

[24] Khanna A, Shetty VK (2014) Solar light induced photocatalytic degradation of reactive blue 220 (rb-220) dye with highly efficient Ag@TiO_2 core-shell nanoparticles: a comparison with UV photocatalysis. Sol. Energy 9967–76.

[25] Haber J, Pamin, K, Matachowski L, Mucha D (2003) Catalytic performance of the dodecatungsto phosphoric acid on different supports. Appl. Catal. A. 256;141-152.

[26] Shinde, PS, Shinde, CH, Bhosale, KY, (2011) Zinc oxide mediated heterogeneous photocatalytic degradation of organic species under solar radiation, J. Photochem. Photobiol. B: Biol. 104425.

[27] Shinde SS, Bhosale CH, Rajpure KY (2011) Photocatalytic activity of sea water using TiO_2 catalyst under solar light. J. Photochem. Photobiol. B: Biol. 10;111.

[28] Amornpitoksuk P, Suwanboon S, Sangkanu S, Sukhoom A, Wudtipan J, Srijan K, Kaewtaro S (2011) Synthesis, photocatalytic and antibacterial activities of ZnO particles modified by deblock. copolymer. Power Tech. 212;432.

[29] Chiua WS, Khiewa PS, Clokea M, Isaa D, Tana TK, Radimanb S, Abd-Shukorb R, Abd-Hamidb MA, Huangc NM, Limd HN, Chiac CH (2010) Photocatalytic study of two-dimensional ZnO nanopellets in the decomposition of methylene blue. Chem. Eng. J. 158;345.

[30] Sun JH, Dong SY, Wang YK, Sun SP (2009) Preparation and photocatalytic property of a novel dumbbell-shaped ZnO microcrystal photocatalyst. J. Hazard. Mater. 172;1520.

[31] Khodja AA, Sehil T, Pilichowski JF, Boule P (2001) Photocatalytic degradation of 2-phenylphenol on TiO_2 and ZnO in aqueous suspensions. J. Photochem. Photobiol. A: Chem. 141;231.

[32] Vinod GK, Kamat PV (1995) Enhanced rates of photocatalytic degradation of an azo dye using SnO_2/TiO_2 coupled semiconductor thin films. Envorn. Sci.

Technol.29;841.
[33] Hoffmann MR., Martin ST, Choi W, Bahnemann DW (1995) Environmental Applications of Semiconductor Photocatalysis. Chem. Rev. 95;69–96.
[34] Herrmann JM (1999). Heterogeneous photocatalysis: Fundamentals and applications to the removal of various types of aqueous pollutants. Catal. Today. 53;115–129.
[35] Pandey N, Shukla S K, and Singh NB (2017) Water purification by polymer nanocomposites: an overview. Nanocomposites. 3;47–66,
[36] Mauro A, Cantarella M, Nicotra G. et al (2017) Novel synthesis of ZnO/PMMA nanocomposites for photocatalytic applications. Sci. Rep.7;1–12,
[37] Sabri M, Habibi-Yangjeh A, Chand H. (2021) Correction to: heterogeneous photocatalytic activation of persulfate ions with novel ZnO/$AgFeO_2$ nanocomposite for contaminants degradation under visible light. J. Mater. Sci. Mater. Electron.; 32;11334-5.
[38] Borhade AV, Tope DR, Uphade BK. (2012) An efficient photocatalytic degradation of methyl blue dye by using synthesised PbO nanoparticles. J. Chem.; 9;11.
[39] Agrawal S, Azra P, Azam A, (2016) vJ. Magnet. Magn. Mater.414;144–152.
[40] Francisco TLM, Marcus ARM, Cassio M and Jose MS, (2016) The Scherrer equation and the dynamical theory of X-ray diffraction Acta Cryst. A72.
[41] Barjasteh-Moghaddam M, Habibi-Yangjeh, A, (2011) Effect of operational parameters on photodegradation of methylene blue on ZnS nanoparticles prepared in presence of an ionic liquid as a highly efficient photocatalyst. J. Iran. Chem. Soc. 8;S169–S175.
[42] Liu, X, Wang, Z, Wu, Y, Liang, Z, Guo, Y, Xue, Y, Cui H (2019) Integrating the Z-scheme heterojunction into a novel Ag_2O@rGO@reduced TiO_2 photocatalyst: Broadened light absorption and accelerated charge separation co-mediated highly efficient UV/visible/NIR light photocatalysis. *J. Colloid Interface Sci. 538*;689–698.
[43] Nguyen, C.H, Fu, C.C, Juang R.S (2018) Degradation of methylene blue and methyl orange by palladium-doped TiO_2 photocatalysis for water reuse: Efficiency and degradation pathways. J. Clean. Prod. *202*;413–427.
[44] Zhu C, Wang L, Kong L, Yang X, Zheng S, Chen F, Maizhi F, Zong H (2000) Photocatalytic degradation of azo dyes by supported TiO_2 UV in aqueous solution. *Chemosphere 41*;303–309.
[45] Senobari S, Nezamzadeh-Ejhieh (2020) A novel ternary nano-composite with a high photocatalyitic activity: characterization, effect of calcination temperature and designing the experiments. J. Photochem. Photobiol. A. 394:112455.
[46] Shankar MV, Anandan S, Venkatachalam N, Arabindoo B, Murugesan V (2004) Novel thin film reactor for photocatalytic degradation of pesticides in an aqueous solution. J. Chem. Technol. Biotechnol.79;1279–85.
[47] Sun H, Cao L, Lu L (2011) Magnetite/reduced graphene oxide nanocomposites: One step solvothermal synthesis and use as a novel platform for removal of dye pollutants. Nano Res.4;550–562.
[48] Huang J, Song H, Chen C, Yang Y, Xu N, Ji X, C. Li and You J.A (2017) Synthesis of N-Doped TiO_2 nanoparticles caged in MIL-100 (Fe) for photocatalytic degradation of organic dyes under visible light irradiation. J. Environ. Chem. Eng. 5;2579–2585.
[49] Salvi N, Banu1 R, Ameta C, Ameta R, Pinki B Punjabi (2021) Enhanced photocatalytic degradation of Nigrosin dye from its aqueous solution using $La_2Ce_2O_7$ nanoparticles. Indian J. Chem. Technol. 28;172-179.
[50] Mahadwad OK, Parikh PA, Jasra RV and Patil C (2011) Photocatalytic degradation of reactive black-5 dye using TiO_2 impregnated ZSM-5. Bull. Mater. Sci. 34;551–556.
[51] Akash T, Gidde MR (2014) Decolourization of Nigrosin WS (AB2) dye by solar photo-fenton process. Int. J. Sci. Technol. Educ. Res. 2;68.
[52] Gadekar LS, Arbad BR, Lande MK (2010) Eco-friendly synthesis of benzimidazole derivatives using solid acid scolecite catalyst. Chin. Chem. Lett. 21;1053.